ACS APPLIED MATERIALS & INTERFACES

Research Article

www.acsami.org

Reducing Regioisomers of Fullerene-Bisadducts by Tether-Directed Remote Functionalization: Investigation of Electronically and Sterically Isomeric Effects on Bulk-Heterojunction Solar Cells

Ming-Hung Liao, Yin-Yu Lai, Yu-Ying Lai, Yen-Ting Chen, Che-En Tsai, Wei-Wei Liang, and Yen-Ju Cheng*

Department of Applied Chemistry, National Chiao Tung University 1001 Ta Hsueh Road, Hsin-Chu, 30010 Taiwan

Supporting Information

ABSTRACT: C_{60} bis-adduct containing a mixture of regio-isomers with different LUMO energy levels and steric geometries could greatly affect the morphological and bulk properties. To investigate the regio-isomer effect on solar cell performance, we have successfully designed and synthesized a regio-selective 4-acetatephenyl-4′-methylphenylmethano C_{60} bis-adduct (S-APM-CBA) by "tether-directed remote functionalization" strategy and a random 4-acetatephenyl-4′-methylphenylmethano C_{60} bis-adduct denoted as R-APM-CBA by traditional cyclopropanation. The dramatic reduction in the number of regio-isomers in S-APM-CBA is confirmed by the ^{1}H NMR and HPLC measurements and theoretical calculation. Compared to the R-APM-CBA-based device with a J_{sc} of 6.63 mA/cm^2, an FF of 44.3% and a PCE of 2.46%, the device using S-APM-CBA yielded a much lower J_{sc} of 1.48 mA/cm^2, an FF of 32.2%, and a PCE of 0.38%. Consistently, the electron-only device using S-AMP-CBA exhibited lower electron mobility than the R-AMP-CBA-based device. These results imply that the electronic shallow-trap effect ascribed to the LUMO energy variations turned out to be insignificant in the AMP-CBA system. The lower efficiency and mobility of S-AMP-CBA might due to the assumption that the most probable *trans*-4-III isomer in S-AMP-CBA prevents the intermolecular facial contact of fullerenes, thereby hindering the electron transporting. Furthermore, the nanomorphology of S-AMP-CBA and R-AMP-CBA active layers could be different because of their different three-dimensional structures. This research demonstrated that steric effect of regio-isomers in a given C_{60} bis-adduct is more crucial than electronic shallow-trap effect.

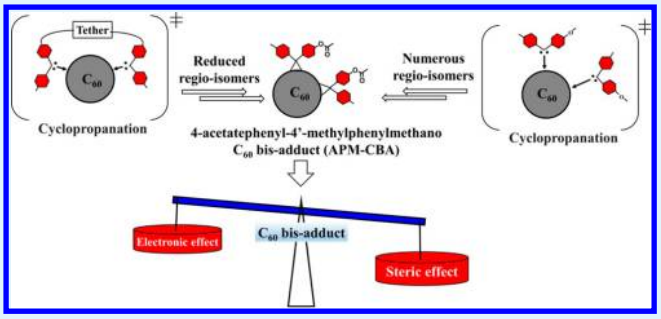

KEYWORDS: *regioisomers, bis-adducts, tether, bulk-heterojunction, solar cells, shallow-trap effect*

INTRODUCTION

Research on polymer solar cells (PSCs) has attracted tremendous scientific and industrial interest and attention in recent years.[1−9] The power conversion efficiency (PCE) of a photovoltaic device is determined by open-circuit voltage (V_{oc}), short-circuit current density (J_{sc}), and fill factor (FF). Increasing V_{oc} is one of the approaches to improve PCEs. The magnitude of V_{oc} value is generally proportional to the energy difference between the highest occupied molecular orbital (HOMO) energy level of the donor and the lowest unoccupied molecular orbital (LUMO) level of the acceptor.[10−12] Therefore, either raising the LUMO level of the fullerene material or lowering the HOMO level of the polymer can obtain higher V_{oc}. A straightforward strategy is to design new fullerene-based materials that possess intrinsically high-lying LUMO energy levels. Introduction of electron-donating groups on the addend of the fullerenes has been attempted to modulate the LUMO energy levels.[13−16] However, the changes in LUMO energy level of fullerene derivatives are too small to affect the V_{oc} because of the fact that the through-space interaction without direct π-conjugation is negligible. Development of bis-adduct C_{60} materials has become a more practical approach.[17−32] The double functionalization on the C_{60} core structure to reduce the electron delocalization in the C_{60} makes bis-adduct C_{60} derivatives have larger electrochemical reduction potentials and thus higher-lying LUMO levels. For example, the bis$PC_{61}BM$ with 56 π-electrons exhibits higher LUMO level by ca. 0.1 eV than the $PC_{61}BM$ with 58 π-electrons. Consequently, the V_{oc} of the P3HT:bis$PC_{61}BM$-based device improves to 0.73 V compared to the P3HT:$PC_{61}BM$-based device with V_{oc} of 0.6 V. Based on the strategy, many fullerene bis-adduct derivatives, such as bis$PC_{61}BM$, $IC_{60}BA$, $IC_{70}BA$, and DMPCBA, have been developed and applied in the PSCs.[17,18,20,28]

Despite that saturating fullerene is beneficial for obtaining high V_{oc}, double functionalization on the core of fullerene in a random fashion inevitably generates a mixture of regio-isomers

Received: October 11, 2013
Accepted: December 17, 2013
Published: December 17, 2013

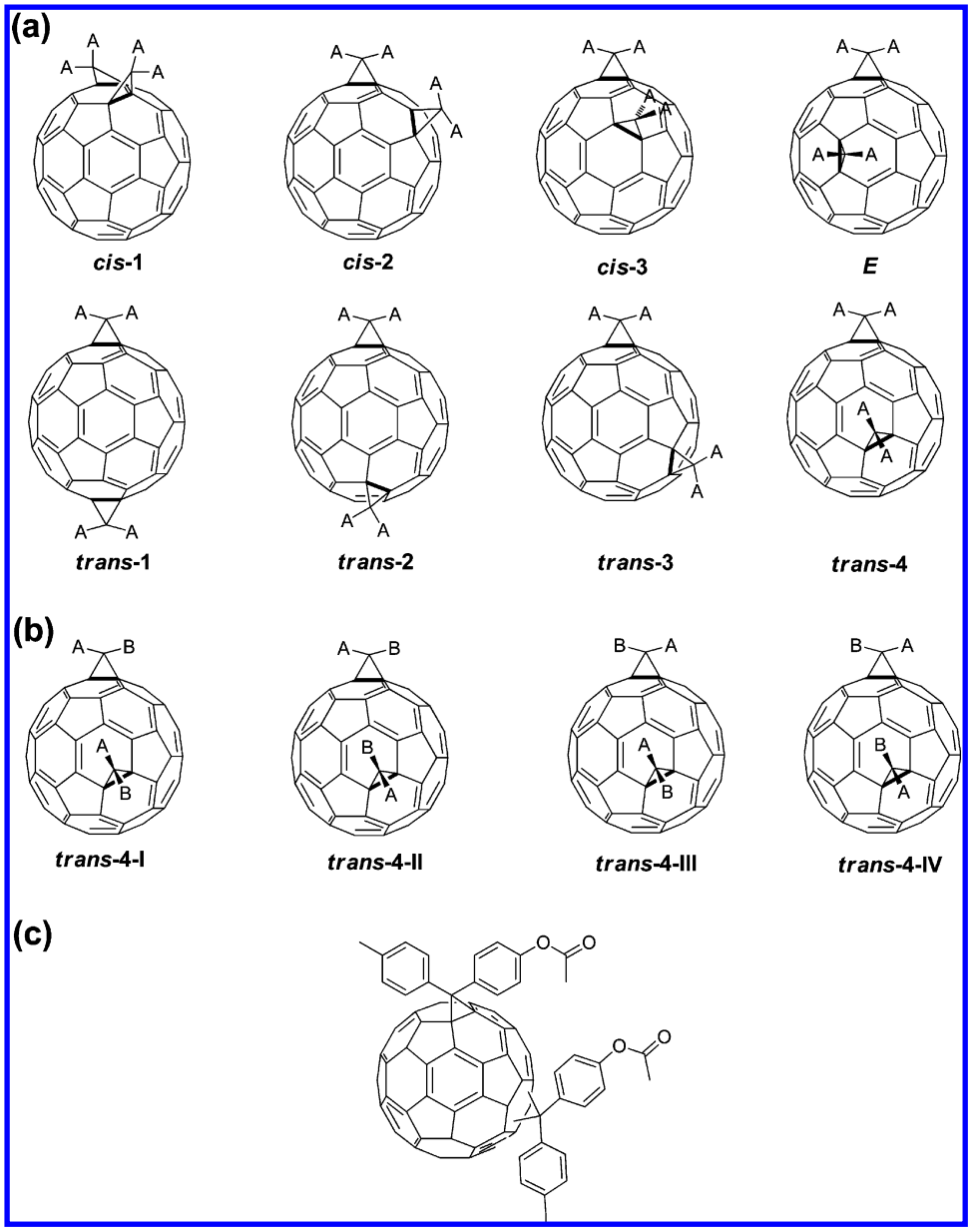

Figure 1. (a) Eight possible regio-isomers of a C_{60} bis-adduct substituted with a symmetrical addend, (b) four possible stereoisomers of *trans*-4 bis-adduct functionalized with an unsymmetrical addend, (c) chemical structure of APM-CBA.

that are difficult to isolate by typical chromatography. The synthesis of mixtures of fullerene bis-adduct suffers from batch-to-batch reproducibility, because the isomer ratio and distribution are highly dependent on synthetic conditions such as temperature, reaction time, and concentration of the reactants.

For two symmetrical A_2C-addends (two A substitutents on the carbon of cyclopropane shown in Figure 1a) functionalized on C_{60} through cyclopropanation reaction, there are eight possible regio-isomers with different substituent locations.[33] When the two A_2C-addends are located on the same hemisphere, there are three possible isomers defined as *cis*-1, *cis*-2, and *cis*-3. Similarly, if the two A_2C-addends are attached on opposite hemispheres, four possible isomers, denoted as *trans*-1, *trans*-2, *trans*-3, and *trans*-4, are generated. When one A_2C-addend is functionalized on the equator of the fullerene sphere, the only one possible isomer is defined as *E*. If addend is unsymmetrical (substitutents are A and B), more possibilities are generated; for instance, 4 different stereoisomers are possible in the *trans*-4 configuration (*trans*-4-I, *trans*-4-II, *trans*-4-III, *trans*-4-IV in Figure 1b). Overall, there will be at most 27 probable regio-isomers and stereoisomers (see the Supporting Information for 27 detailed structures). Because the structures of C_{60} bis-adduct are not well-defined, the structural change of isomers could lead to different steric and electronic properties, which in turn affects device performance.

First, the different isomeric structure of bis-adducts may alter the molecular packing and thereby the resultant morphology.[34] Moreover, each regio-isomer is expected to possess different reduction potentials. The existence of variations in the LUMO energy levels of isomers may cause energetic traps (i.e., shallow traps) which are supposed to have negative impact on J_{sc} and FF. Although the shallow-trap effect has been speculated to be detrimental, the in-depth and detailed studies are still limited.[35−39] To investigate whether the shallow-trap effect, resulting from a bunch of regioisomers, is important in affecting

device performance or not, a straightforward method is to reduce the number of regioisomers of a given C_{60}-bisadduct by chemical control. However, it is synthetically very challenging. To regulate specific regio-isomers within C_{60} bis-adduct, Diederich et al. introduced a "tether-directed remote functionalization" (TDRF) based on the idea that two addend groups are covalently attached on a tether moiety.[40−46] After the tether-induced regio-selective reaction with C_{60}, the tether group can be chemically removed to resume the specific fullerene bis-adduct. Herein, we attempt to investigate the isomeric effect of a new C_{60} bis-adduct, APM-CBA, where two (4-acetatephenyl)-4-methylphenyl methano (APM) moieties are functionalized on a C_{60} through cyclopropanation (Figure 1c). We deliberately synthesized APM-CBA by means of two independent approaches. Random APM-CBA (R-APM-CBA) was prepared by the standard cyclopropanation, whereas regio-selective APM-CBA (S-APM-CBA) was synthesized by the TDFR strategy. The difference in numbers of isomers between R-APM-CBA and S-APM-CBA provides a model to investigate the isomeric (i.e., shallow-trap and steric) effect in bulk heterojunction solar cells.

RESULTS AND DISCUSSION

The molecular design is shown in Figure 2. Two diphenylmethano-based anchoring groups are linked with a tether group. The tosylhydrazone functional groups are used to undergo cyclopropanation reaction with fullerene. The length and rigidity of a tether moiety play an important role in governing regio-selectivity of the two anchoring groups on C_{60}. By careful manipulation, the two anchoring groups can be located in the same hemisphere (*cis* form) or opposite hemisphere (*trans* form) of C_{60}. 1,6-Hexylene and 1,4-xylyl moieties are selected as a soft tether and an rigid tether, respectively, to connect two 4-methylbenzophenone tosylhydrazone addends together (Scheme 1 and Figure 2) for preliminary study.

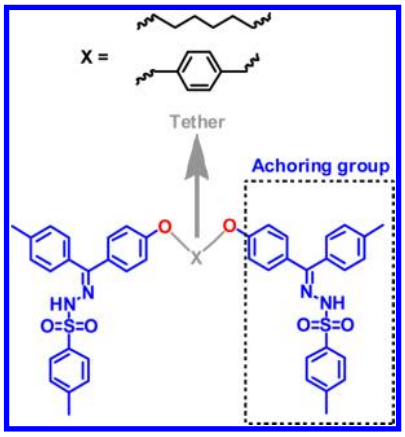

Figure 2. Rigid and soft tether moieties in this research for tether-directed remote functionalization.

Synthesis. The synthesis of S-APM-CBA is shown in Scheme 1. Friedel−Craft acylation of 4-methoxy benzoyl chloride with toluene afforded 4-methoxy-4′-methylbenzophenone (**1**).[47] Demethylation of compound **1** by boron tribromide led to 4-hydroxy-4′-methylbenzophenone (**2**). Under basic conditions, compound **2** was reacted with a tether molecule, 1,4-bis(bromomethyl) benzene or 1,6-dibromohexane, to give **3a** or **3b**, respectively. Condensation of compound **3a** and **3b** with *p*-toluenesulfonhydrazide furnished bis-tosylhydrazone **4a** and **4b** in good yield, respectively. In the presence of sodium hydride at 130 °C, cyclopropanation of tosylhydrazone groups in compound **4a** and **4b** with C_{60} led to the formation of tether-directed C_{60} bis-adduct intermediate **5**. Dealkylation of compound **5a** by BBr_3 successfully yielded compound **6** with two hydroxy groups that were allowed to react with acetyl chloride to yield the desired S-APM-CBA.

On the other hand, the synthesis of R-APM-CBA is shown in Scheme 2. Compound **7** reacted with C_{60} to yield C_{60} bis-adduct **8**. In a similar manner, demethylation of compound **8** followed by acylation generated the final R-APM-CBA.

Proton NMR and HPLC Measurements. We first studied the effect of the different tether linkers on the regio-selectivity by measuring NMR spectra of compound **5a** and **5b** shown in a and b in Figure S1 in the Supporting Information, respectively. Compared to **5b**, **5a** with *p*-xylene as the tether exhibited less complicated peaks in the NMR spectrum, implying that the rigid 1,4-xylyl tether results in less regio-isomers than the soft *n*-hexyl tether. As a result of the better regio-selectivity, we selected only compound **5a** for the following synthetic steps to make the final S-APM-CBA. The NMR spectra of S-APM-CBA and R-APM-CBA were measured to evaluate the effectiveness of tether-directed approach, as shown in panels a and b in Figure 3, respectively. Again, R-APM-CBA showed very complicated peaks from 2.0 to 2.6 ppm, which ascribed to the methyl groups of toluene as well as the methyl groups of ester. In contrast, S-APM-CBA showed much simpler and clearer peaks. Similar phenomena were observed in the aromatic region from 7 to 8.5 ppm, indicating that S-APM-CBA synthesized by the TDRF approach indeed contains many fewer regio-isomers than R-APM-CBA made by the typical method.

The stereochemistry of two 4-acetatephenyl-4′-methylphenylmethano groups in S-APM-CBA is determined by its precursor **5a**. S-APM-CBA should inherit the stereochemistry of **5a** and the number of stereoisomers should be identical for S-APM-CBA and **5a**. **5a** was then used to estimate the possible isomers of S-APM-CBA. With the help of a molecular-structure visualization program-GaussView 5.0, we found that **5a** has at most 7 stereoisomers on account of the fact that the presence of the 1,4-xylyl tether forbids sterically the formation of the other isomers. The optimized structures of the 7 isomers are depicted in Figure 4, which includes *cis*-2-I, *cis*-2-III, *cis*-3-I, *cis*-3-II, *E*-II, *E*-III, and *trans*-4-III. Roman numerals are used to symbolize the stereoisomers resulting from the same class of regio-isomer illustrated in Figure 1 (also see the Supporting Information, Figure S1, for nomenclature). Since the interconversion between these isomers is nearly impossible, the distribution of isomers for **5a** should be govern primarily by the activation barrier for the reaction from **4a** to **5a** among isomers. For this reaction, we reason that 4a would first react with C_{60} to form a monoadduct with exclusive stereochemistry. Subsequently, the monoadduct would undergo another cycloaddition to give **5a**. The second cycloaddition is expected to be the rate-determining step for this reaction and therefore the energy difference in the transition state for the second cycloaddition among the isomers would determine the relative product distribution. Furthermore, it can be envisaged that the energy difference between either the transition states or the resultant isomers would highly correlate with the strain resulting from the cyclic tether-addend. In light of this assumption, the energy difference between the isomers could

Scheme 1. Synthesis of S-APM-CBA by the Tether-Directed Remote Functionalization

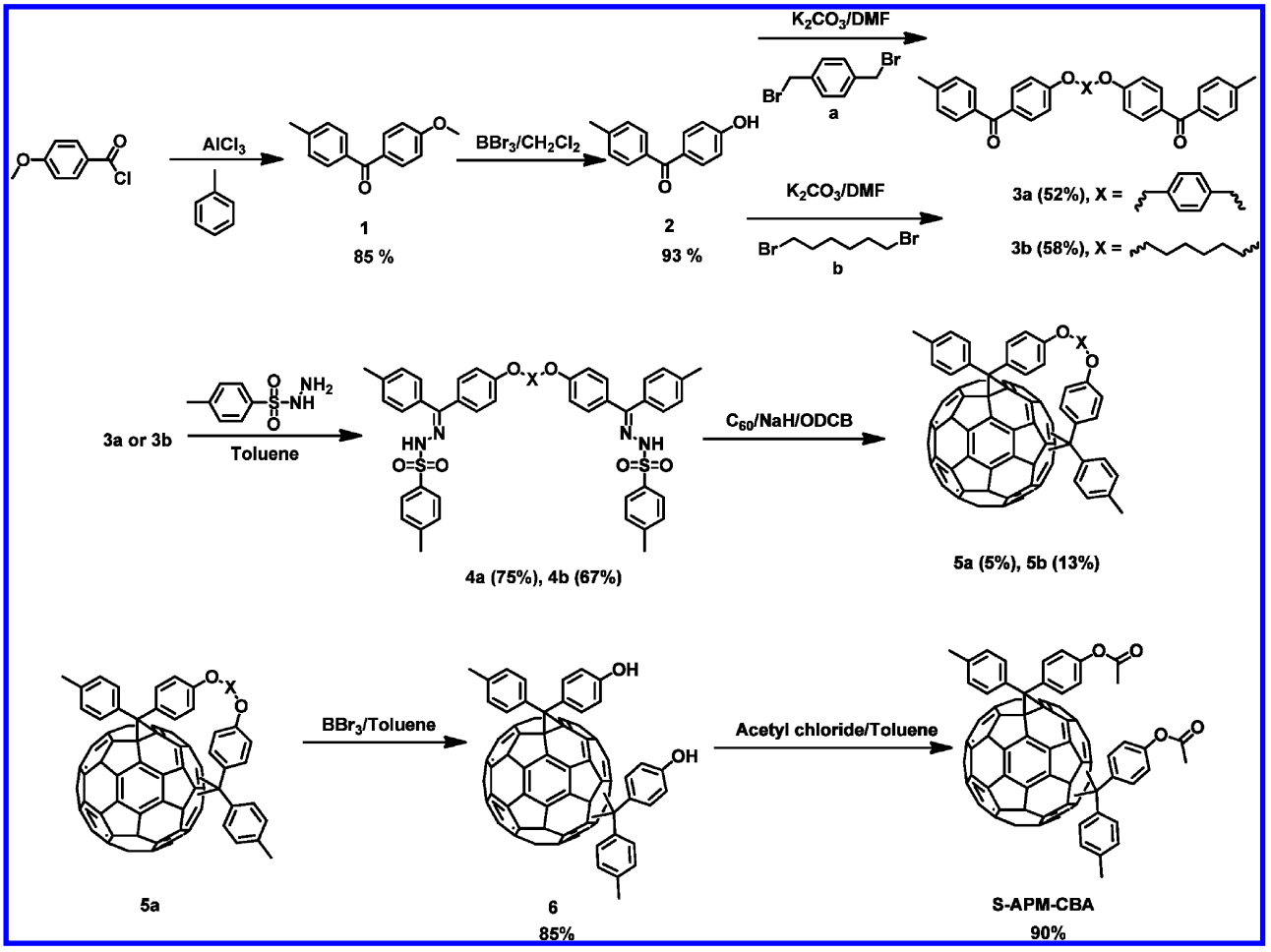

Scheme 2. Synthetic Route of the R-APM-CBA

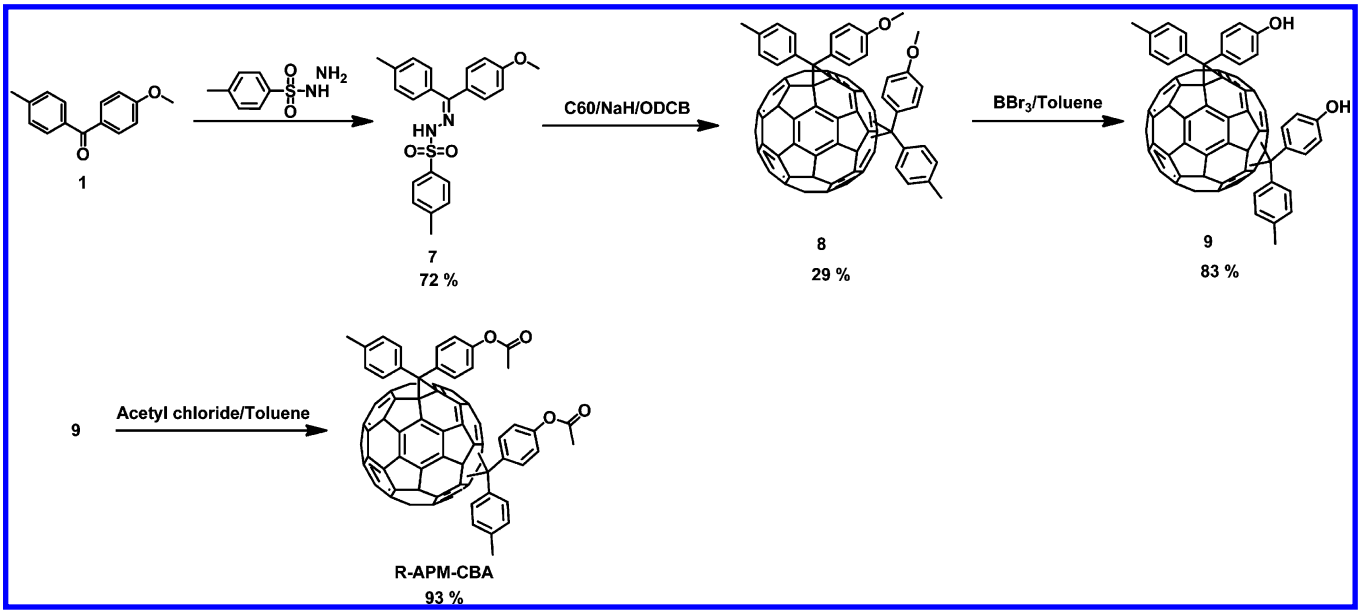

be used to roughly approximate the energy difference between the transition states and thus the distribution of isomers. Theoretical calculations on the PM3 level of theory were employed to calculate the electronic energy and Gibbs free energy (25 °C in kcal mol^{-1}) for the 7 isomers. *Trans*-4-III has the lowest energy which is set as zero for calibration. The electronic energy and Gibbs free energy relative to *trans*-4-III for the rest of **5a** isomers (i.e., ΔE and ΔG) are shown in Table 1. It was found that there is no significant difference between the electronic energy and Gibbs free energy. We therefore

dx.doi.org/10.1021/am404485t | *ACS Appl. Mater. Interfaces* 2014, 6, 996−1004

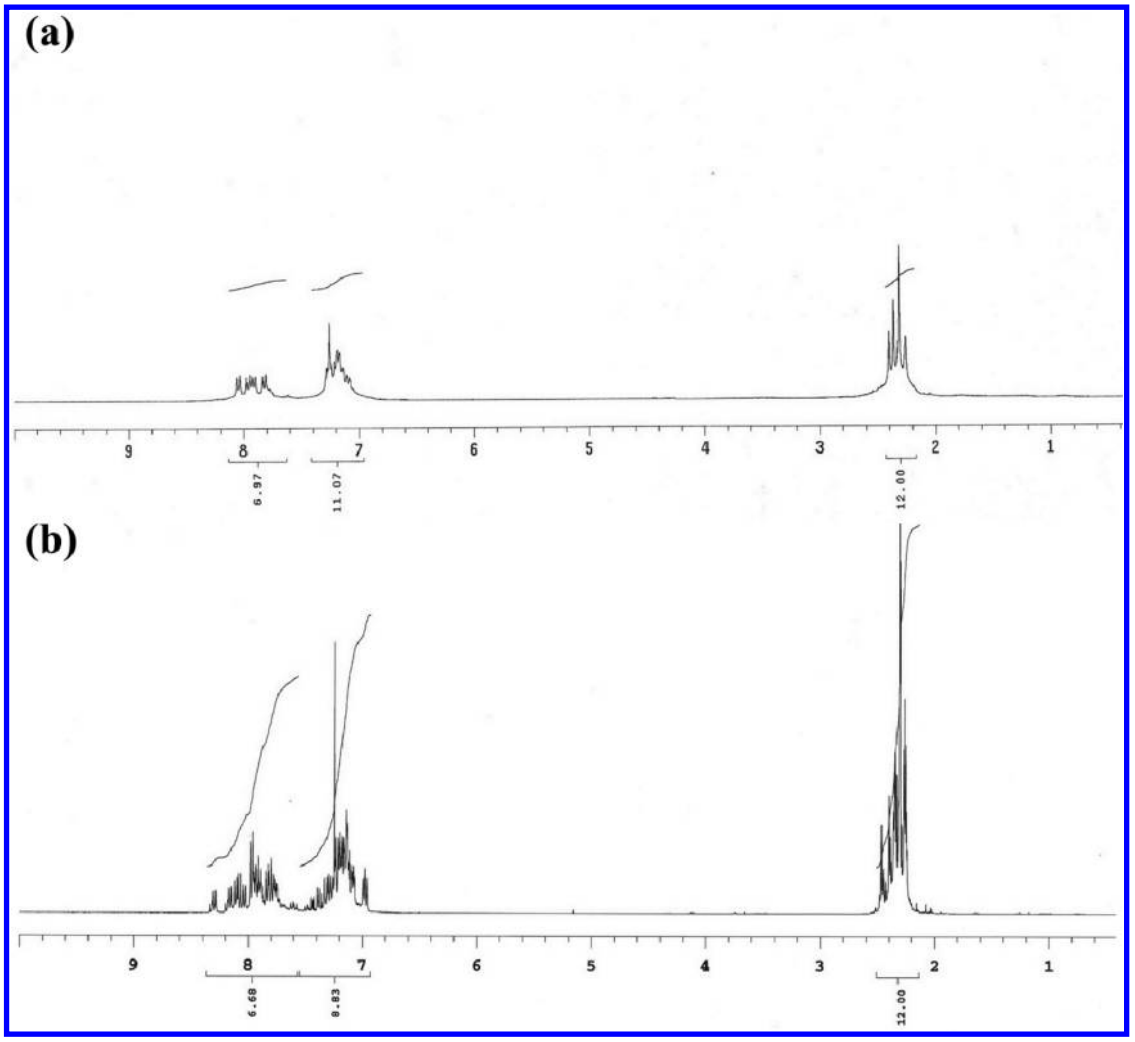

Figure 3. ^{1}H NMR spectrum of (a) S-APM-CBA and (b) R-APM-CBA.

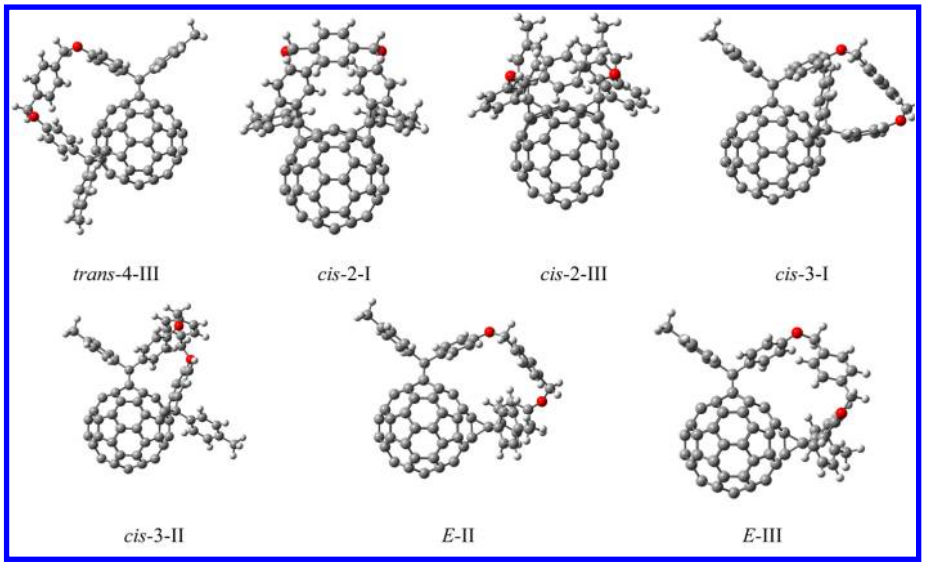

Figure 4. Optimized geometries of 7 isomers of **5a** at the PM3 level of theory. Red, oxygen; gray, carbon; light-gray, hydrogen.

choose the electronic energy for the following discussion. Comparison of the optimized geometries with the corresponding electronic energies revealed that an isomer with highly strained conformation also possesses high energy. The energy of an isomer appears to be determined by the strain of the cyclic addend. The electronic energy of the isomers follows the order: *trans*-4-III < *cis*-2-I < *cis*-2-III < *cis*-3-II < *E*-III < *E*-II < *cis*-3-I. On the basis of the calculated energies, *trans*-4-III, *cis*-2-

dx.doi.org/10.1021/am404485t | *ACS Appl. Mater. Interfaces* 2014, 6, 996−1004

Table 1. Electronic Energy Difference (ΔE) and Gibbs Free Energy Difference (25 °C) (ΔG) in kcal mol^{-1} Relative to *trans*-4-III for the 5a Isomers

	trans-4-III	*cis*-2-I	*cis*-2-III	*cis*-3-I	*cis*-3-II	*E*-II	*E*-III
ΔE	0	1.85	4.02	16.09	7.29	12.74	9.33
ΔG	0	1.30	4.50	17.90	7.40	12.50	11.40

I, and *cis*-2-III are the more likely isomers for **5a**. The computational results support that the tether-directed remote functionalization can significantly reduce the number of regio-isomers.

High-performance liquid chromatography (HPLC) was also employed to estimate the regio-isomers of bis-adduct C_{60}. The HPLC chromatogram of R-APM-CBA showed very broad distribution containing at least 12 distinct peaks ranging from 20 to 60 min retention time (Figure 5). To roughly identify the

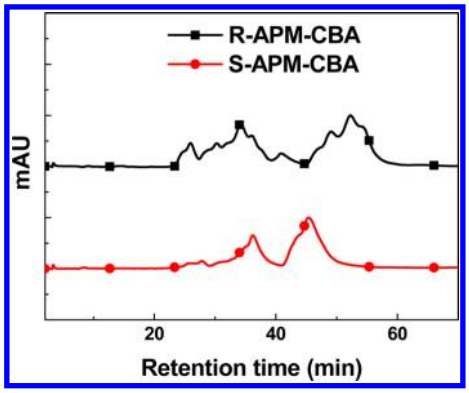

Figure 5. High-performance liquid chromatography (HPLC) chromatogram of R-APM-CBA and S-APM-CBA using toluene and ethyl acetate (4:1, v/v) as eluents at a flow rate of 1 mL/s.

composition of the isomers in the normal phase of the HPLC, it is expected that the short-time signals belong to the trans-based isomers with lower polarity, whereas the long-time signals are assigned to the cis-based isomers with higher polarity. In contrast, the S-APM-CBA chromatogram showed only two major signals peaked at 38 and 47 min without observation of signals around shorter time (22−33 min) and longer time (50−60 min). These results are fairly consistent with the theoretical calculations suggesting that *trans*-4-III, *cis*-2-III, *cis*-3-I, and *cis*-3-II are the most probable isomers whose polarities are relatively moderate among the full isomers. HPLC data again indicated that a bis-adduct C_{60} with significantly reduced regio-isomers can be achieved by applying the tether-directed approach.

Optical Properties. The optical absorption of R-APM-CBA, S-APM-CBA and $PC_{61}BM$ was characterized in THF with a concentration of 1×10^{-5} M (Figure 6). The absorption profiles of R-APM-CBA and S-APM-CBA without shoulders around 260 and 330 nm are dissimilar to that of $PC_{61}BM$. Interestingly, the absorption intensity of R-APM-CBA is much higher than that of S-APM-CBA under the same concentration, indicating that different regio-isomers can possess very distinct absorption coefficients.[34,42,48]

Electrochemical Properties. The electrochemical properties of the R-APM-CBA and S-APM-CBA were investigated by cyclic voltammetry (CV) in Figure 7. The cyclic voltammetry showed three well-defined and reversible redox waves in the potential ranging from 0 to −2.5 V. In the negative potential

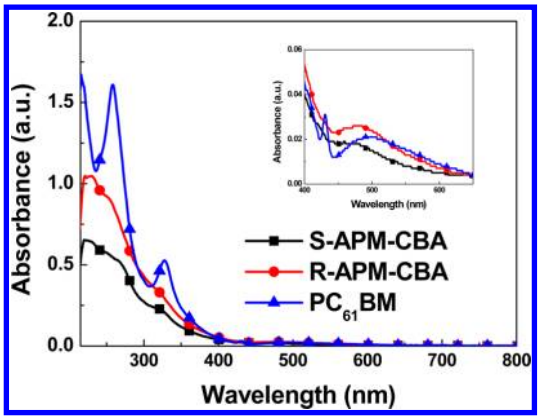

Figure 6. Absorption spectra of S-APM-CBA, R-APM-CBA and PC61BM in THF solution under the concentration of 1×10^{-5} M. Inset: Enlarged absorption spectra from 400 to 800 nm.

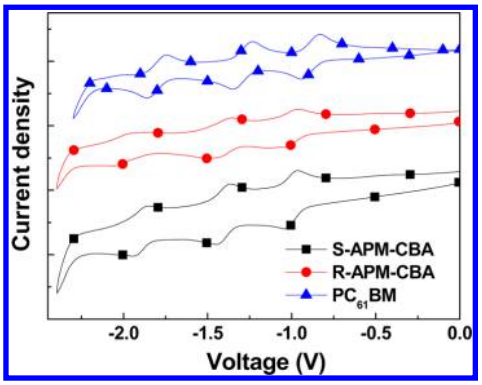

Figure 7. Cyclic voltammetry of R-APM-CBA, S-APM-CBA, and $PC_{61}BM$ at a scan rate of 100 mV/S.

region, R-APM-CBA and S-APM-CBA showed similar reduction potentials which shift more negatively by 0.15 eV compared to $PC_{61}BM$. The LUMO energy levels of S-APM-CBA, R-APM-CBA, and $PC_{61}BM$ are estimated to be −3.77, −3.76, and −3.91 eV, respectively. The higher LUMO energy level of the bis-adducts would be advantageous for improving V_{oc}. Notably, the energetic difference of 0.01 eV between S-APM-CBA and R-APM-CBA might cause the shallow-trap effect. Besides, we found that the CV profile of R-APM-CBA is slightly broader than that of S-APM-CBA, which is consistent with the fact that R-APM-CBA contains more regio-isomers with small variations of energetic energy levels.[30]

Table 2. Onset Reduction Potentials and LUMO Energy Levels of Fullerene Derivatives

fullerene derivatives	E_1[a] (V)	E_2 (V)	E_3 (V)	LUMO (eV)
S-APM-CBA	−0.92	−1.33	−1.83	−3.77
R-APM-CBA	−0.94	−1.33	−1.85	−3.76
$PC_{61}BM$	−0.81	−1.22	−1.73	−3.91

[a]Potential values in this table are versus Ag/Ag^+ reference electrode.

Photovoltaic Characteristics. Bulk heterojunction solar cells with configuration (ITO/PEDOT:PSS/P3HT:fullerene derivatives/Ca/Al) were fabricated and characterized under simulated 100 mW cm^{-2} AM 1.5 G illumination (Figure 8). The device characteristics with the optimal blending ratio are shown in Table 3. The device using P3HT:R-APM-CBA blend (1:1 in wt %) showed a V_{oc} of 0.84 V, FF of 44.3%, and J_{sc} of

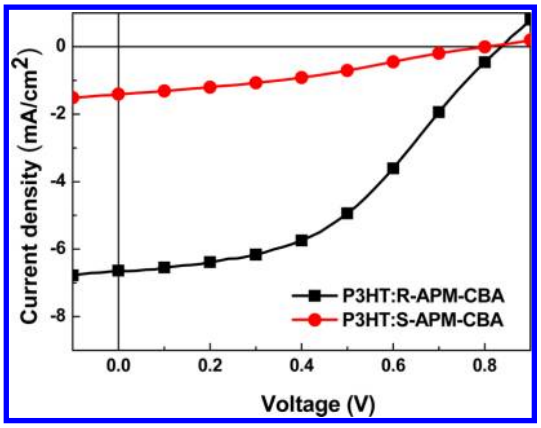

Figure 8. $J-V$ curves of the PSCs based on (ITO/PEDOT:PSS/P3HT:S-APM-CBA or R-APM-CBA (1: 1 wt %)/Ca/Al) under illumination of AM 1.5G (100 mW/cm^2).

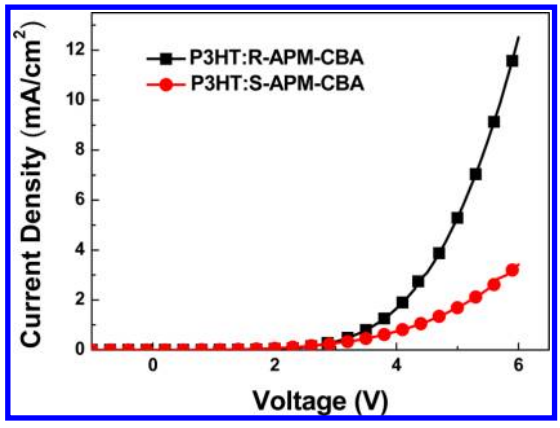

Figure 9. $J-V$ curves of the electron-only devices based on the ITO/ZnO/P3HT:S-APM-CBA or P3HT:R-APM-CBA (1: 1 wt %)/Al configuration.

Table 3. Device Characteristics of (ITO/PEDOT:PSS/P3HT:S-APM-CBA or P3HT:R-APM-CBA (1:1 wt %)/Ca/Al)

acceptor	V_{oc} (V)	J_{sc} (mA/cm^2)	FF (%)	PCE (%)
S-APM-CBA	0.80	1.48	32.16	0.38
R-APM-CBA	0.84	6.63	44.30	2.46

6.63 mA/cm^2, resulting in a PCE of 2.46%. Surprisingly, under similar conditions, the device with S-APM-CBA containing less regioisomers turned out to exhibit a much lower PCE of 0.38% with a V_{oc} of 0.80 V, an FF of 32.16%, and a J_{sc} of 1.48 mA/cm^2. Considering that the only difference between R-APM-CBA and S-APM-CBA is the number of isomers, the inferior device performance of S-APM-CBA implies that the electronic shallow-trap effect in R-APM-CBA is not pronounced. The discrepancy is thus ascribed to the steric effect of the regio-isomers. The different structural geometry of the regio-isomers causes different intermolecular interaction and morphology of the composite. We speculated that the *trans*-4-III isomer where the two addends locate on different hemispheres of C_{60} might sterically suppress the facial contact between the fullerene cages.[36] Therefore, the electron transportation in R-APM-CBA might be significantly hindered within the fullerene phase. On the basis of the speculation, the electron-only devices (ITO/ZnO/P3HT:bisadducts (1:1 in wt%)/Al) were fabricated to study the charge transporting capability of S-APM-CBA and R-APM-CBA-based blends (Figure 9). The R-APM-CBA-based device yielded a mobility of 8.01×10^{-6} cm^2 V^{-1} s^{-1}, which is higher than the corresponding S-APM-CBA-based device by 4-folds (1.8×10^{-6} cm^2 V^{-1} s^{-1}). The smaller electron mobility is responsible for the inferior solar cell performance of S-APM-CBA. As a result, the shallow-trap effect is insignificant in the BHJ solar cells in comparison of the steric effect.

Morphological Study. The morphology of the P3HT:R-APM-CBA and P3HT:S-APM-CBA (1:1 in wt%) blends are studied by atomic force microscope (AFM) and showed in the Figure 10. The surface roughness of P3HT:R-APM-CBA and P3HT:S-APM-CBA thin films are 14.7 and 12.6 nm, respectively. The difference in roughness is probably due to the different composition of the regioisomers of APM-CBA.

CONCLUSIONS

Fullerene bis-adducts with intrinsically high-lying LUMO energy levels are superior N-type materials for PSCs to improve open-circuit voltage. However, double functionalization reaction of fullerene with addend moieties inevitably creates a mixture of regioisomers. The fullerene bis-adduct isomers having different LUMO energy levels and steric geometries could greatly influence molecular and morphological properties in PSCs. To investigate the isomer effect of a C_{60} bisadduct, random (4-acetatephenyl)-4-methylphenyl methano C_{60} bis-adduct (R-APM-CBA) was synthesized by the traditional reaction, whereas regio-selective S-APM-CBA was achieved by a "tether-directed remote functionalization" strategy. The significant reduction in the number of regioisomers in S-APM-CBA is manifested by the ^{1}H NMR, HPLC measurements and theoretical calculation. Surprisingly, the PSC using S-APM-CBA turned out to yield much lower J_{sc} of 1.48 mA/cm^2 and FF of 32.16% compared to the R-APM-CBA-based device with J_{sc} of 6.63 mA/cm^2 and FF of 44.3%. Consistently, the electron-only device of S-AMP-CBA showed much lower electron mobility than that of R-AMP-CBA by 4-folds. These results imply that the electronic shallow traps as a result of the LUMO energy variations are insignificant in the AMP-CBA system. The structural geometry of *trans*-4-III, the most probable isomer in S-AMP-CBA, might prevent the intermolecular facial contact, hindering the electron transporting. This research demonstrated that the steric effect of regioisomers in a given C_{60} bis-adduct is more crucial than the electronic shallow-trap effect. Reducing isomers of C_{60} bis-adduct can be achievable by TDRF; however, targeting a specific bis-adduct isomer with an optimal structural geometry for superior charge-transporting property remains a challenging task. It is envisioned that this model study will pave the way for further research on controlling the properties of the bis-adduct fullerene materials, which plays a key role in making breakthrough of organic solar cells.

EXPERIMENTAL SECTION

Synthesis of Compound 1. A solution of aluminum chloride (2 g, 15 mmol) in dry toluene was added slowly *p*-methoxybenzoyl chloride (2 g, 10 mmol) at 0 °C. The mixture was stirred at room temperature for 10 h. The reaction was quenched by pouring the mixture into ice/water and then extracted with ethyl acetate/H_2O. The crude product was purified by silica column to give the product (hexane:ethyl acetate = 5:1, v/v, 4.2 g, 93%). ^{1}H NMR (300 MHz, $CDCl_3$) δ = 2.44 (s, 3H), 3.89 (s, 3H), 6.96 (d, J = 9.0 Hz, 2H), 7.27 (d, J = 7.8 Hz, 2H), 7.68 (d, J = 7.8 Hz, 2H), 7.81 (d, J = 9.0 Hz, 2H).

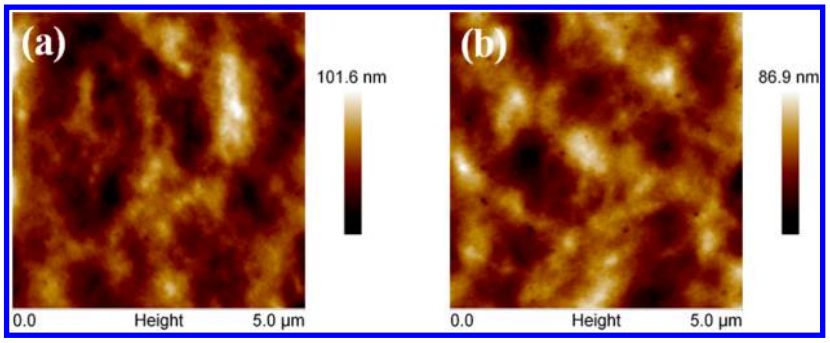

Figure 10. AFM height images of (a) P3HT:R-APM-CBA and (b) P3HT:S-APM-CBA (1:1 in wt %) blend films.

Synthesis of Compound 2. A solution of compound **1** (10 g, 44 mmol) in dry dichloromethane was slowly added boron tribromide (1M, 44.2 mL, 44.2 mmol) at 0 °C. The mixture was stirred at room temperature for 24 h. The resulting solution was poured into ice/water and then extracted with CH_2Cl_2/H_2O. The organic phase was dried by anhydrous $MgSO_4$, and then concentrated in vacuo. The crude product was purified by silica column to give the product (hexane:ethyl acetate = 1: 1, v/v, 8.4 g, 90%). ^{1}H NMR (300 MHz, $CDCl_3$) δ = 2.43 (s, 3H), 6.63 (s, 1H), 6.92 (d, J = 8.4 Hz, 2H), 7.27 (d, J = 8.1 Hz, 2H), 7.68 (d, J = 8.1 Hz, 2H), 7.76 (d, J = 8.4 Hz, 2H). EI-MS (m/z): 212.

Synthesis of Compound 3a. A mixture of compound **2** (1 g, 4.7 mmol), 1,4-bis(bromomethyl)benzene (0.62 g, 2.36 mmol), and NaH (0.34 g, 14 mmol) was dissolved in anhydrous DMF (20 mL) and stirred under a N_2 atmosphere at room temperature for 24 h. The resulting mixture was extracted with CH_2Cl_2/H_2O. The organic layer was dried by anhydrous $MgSO_4$ and concentrated in vacuo. The residue was washed by hexane for several times to afford a white solid (0.99 g, 40%). ^{1}H NMR (300 MHz, $CDCl_3$) δ = 2.44 (s, 6H), 5.17 (s, 4H), 7.03 (d, J = 8.7 Hz, 4H), 7.28 (d, J = 7.8 Hz, 4H), 7.49 (s, 4H), 7.68 (d, J = 8.1 Hz, 4H), 7.81 (d, J = 9 Hz, 4H). FAB-MS (m/z): 526.

Synthesis of Compound 3b. In a similar manner for compound **3a**, compound **3b** was obtained in a 48% yield. ^{1}H NMR (300 MHz, $CDCl_3$) δ = 1.55−1.60 (m, 4H), 1.85−1.89 (m, 4H), 2.43 (s, 6H), 4.06 (t, J = 6.5 Hz, 6H), 6.94 (d, J = 9 Hz, 4H), 7.27 (d, J = 7.2 Hz, 4H), 7.67 (d, J = 8.1 Hz, 4H), 7.80 (d, J = 8.7 Hz, 4H).

Synthesis of compound 4a. A mixture of compound **3a** (3 g, 5.7 mmol) and tosylhydrazide (2.34 g, 0.125 mmol) was dissolved in toluene (100 mL). The solution was refluxed for 12 h. The mixture was concentrated in vacuo and purified by column chromatography on silica gel (hexane: EA = 1:1, v/v). The residue was dissolved in THF (10 mL) and precipitated into hexane (150 mL). The solid compound was filtered off and dried by vacuum (3.98 g, 81%).^{1}H NMR (300 MHz, $CDCl_3$) δ = 2.31−2.43 (m, 12H), 5.05−5.16 (m, 4H), 6.84−7.86 (m, 30H). FAB-MS (m/z): 864.

Synthesis of Compound 4b. In a similar manner, compound **4b** was obtained in a yield of 70%.^{1}H NMR (300 MHz, $CDCl_3$) δ = 1.50−1.58 (m, 4H), 1.79−1.85 (m, 4H), 2.31−2.42 (m, 12H), 3.92−4.07 (m, 4H), 6.76−7.86 (m, 26H). FAB-MS (m/z): 844.

Synthesis of Compound 5a. Compound **4a** (0.36 g, 0.42 mmol), C_{60} (0.3 g, 0.42 mmol), and NaH (0.06g, 2.5 mmol) were dissolved in dry toluene (500 mL) under nitrogen. The resulting mixture was refluxed and stirred for 12 h. The mixture was concentrated in vacuo and then purified by column chromatography (SiO_2, toluene: hexane = 1: 1, v/v). The solid residue was dissolved in the CS_2 and then precipitated into methanol. The solid was filtered off and then washed by methanol for several times. The black compound was dried in vacuum (25 mg, 5%).^{1}H NMR (300 MHz, $CDCl_3$) δ = 2.11−2.42 (m, 6H), 4.95−5.45 (m, 4H), 6.55−7.99 (m, 28H).FAB-MS (m/z): 1215.

Synthesis of Compound 5b. In a similar manner for compound **5a**, compound **5b** was obtained in a yield of 13%. ^{1}H NMR (300 MHz, $CDCl_3$) δ = 1.25−1.62 (m, 8H), 2.32−2.41 (m, 4H), 3.99−4.16 (m, 4H), 6.71−7.99 (m, 16H). FAB-MS (m/z): 1196.

Synthesis of Compound 6. To a solution of compound **5a** (100 mg, 0.08 mmol) in dry dichloromethane was slowly added boron tribromide (1M, 0.32 mL, 0.32 mmol) at 0 °C. The mixture was stirred at room temperature for 6 h. A further quantity of boron tribromide (0.32 mL, 0.32 mmol) was added and the mixture was stirred for extra 12 h. The resulting solution was poured into ice/water and then extracted with CH_2Cl_2/H_2O. The organic phase was dried by anhydrous $MgSO_4$, and then concentrated in vacuo. The crude product was purified by silica column to give the product (toluene: ethyl acetate =1: 2, v/v, 78 mg, 85%). ^{1}H NMR (300 MHz, $CDCl_3$) δ = 2.30−2.44 (m, 6H), 5.07 (s, 2H), 6.76−7.91 (m, 16H). FAB-MS (m/z): 1113.

Synthesis of S-APM-CBA. To a solution of compound **6** (80 mg, 0.072 mmol) in the dry dichloromethane with three drops Et_3N was added acetyl chloride (16.8 mg, 0.216 mmol) at 0 °C. The resulting mixture stirred at room temperature for 12 h. The resulting solution extracted with CH_2Cl_2/H_2O and the organic layer was concentrated in vacuo. The crude product was purified by silica column to give the compound (toluene: ethyl acetate = 10: 1, v/v, 77 mg, 90%).^{1}H NMR (400 MHz, $CDCl_3$) δ = 2.26−2.40 (m, 12H), 7.08−7.28 (m, 8H), 7.81−8.06 (m, 8H).^{13}C NMR (100 MHz, $CDCl_3$) δ = 21.2, 21.3, 25.6, 29.7, 54.8, 68.0, 130.7, 131.0, 131.2, 131.3, 131.5, 131.8, 135.0, 135.7, 136.1, 136.2, 137.0, 137.1, 137.6, 137.8, 137.9, 138.0, 139.7, 140.8, 141.3, 141.9, 142.1, 142.2, 142.7, 143.0, 143.8, 144.6, 144.7, 144.9, 145.1, 145.3, 145.4, 145.6, 145.7, 146.2, 146.6, 146.9, 147.8, 147.9, 150.0, 150.1, 169.1, 169.2. FAB-MS (m/z): 1197.

Synthesis of Compound 7. In a similar manner for compound **4a**, compound **7** was obtained in a yield of 75%.^{1}H NMR (300 MHz, $CDCl_3$) δ = 2.32 and 2.42 (s, 6H), 3.78 and 3.87 (s, 3H), 6.79 (d, J = 6.6 Hz, 2H), 6.96−7.09 (m, 3H), 7.25−7.53 (m, 6H), 7.83 (d, J = 6.3 Hz, 2H). FAB-MS (m/z): 395.

Synthesis of Compound 8. In a similar manner for compound **5a**, compound **8** was obtained in a yield of 35%.^{1}H NMR (300 MHz, $CDCl_3$) δ = 2.17−2.46 (m, 6H), 3.68−3.90 (m, 6H), 6.61−7.32 (m, 10H), 7.37−8.14 (m, 6H). FAB-MS (m/z): 1140.

Synthesis of Compound 9. In a similar manner for compound **6**, compound **9** was obtained in a yield of 93%.^{1}H NMR (300 MHz, $CDCl_3$) δ = 2.04−2.46 (m, 6H), 3.75−5.08 (m, 2H), 6.76−8.20 (m, 16H). FAB-MS (m/z): 1113.

Synthesis of R-APM-CBA. In a similar manner for **S-APM-CBA**, **R-APM-CBA** was obtained in a yield of 87%.^{1}H NMR (400 MHz, $CDCl_3$) δ = 2.08−2.47 (m, 12H), 7.10−8.31 (m, 16H).^{13}C NMR (100 MHz, $CDCl_3$) δ = 21.3, 27.6, 30.0, 51.7, 54.5, 54.8, 56.3, 121.7, 126.0, 127.7, 128.1, 129.5, 129.9, 130.2, 130.7, 131.0, 131.3, 131.8, 132.1, 134.1, 135.0, 135.6, 136.2, 136.5, 137.1, 137.8, 138.7, 139.7, 140.0, 140.6, 140.9, 141.5, 141.8, 142.2, 142.5, 143.0, 143.5, 144.3, 145.3, 145.8, 146.2, 146.5, 147.1, 147.9, 148.8, 149.4, 150.0, 151.0, 169.1. FAB-MS (m/z): 1197.

■ ASSOCIATED CONTENT

Ⓢ Supporting Information

Device fabrication and characterization, NMR spectra, all the possible structures of stereoisomers for a C_{60} bis-adduct, theoretical calculations, hole-only devices, and open circuit light intensity measurement. This material is available free of charge via the Internet at http://pubs.acs.org.

AUTHOR INFORMATION

Corresponding Author

*E-mail: yjcheng@mail.nctu.edu.tw.

Notes

The authors declare no competing financial interest.

ACKNOWLEDGMENTS

We thank the National Science Council and the Ministry of Education, and Center for Interdisciplinary Science (CIS) of the National Chiao Tung University, Taiwan, for financial support. We thank the National Center of High-Performance Computing (NCHC) in Taiwan for computer time and facilities.

REFERENCES

(1) Arias, A. C.; MacKenzie, J. D.; McCulloch, I.; Rivnay, J.; Salleo, A. *Chem. Rev.* **2010**, *110*, 3−24.

(2) Yu, G.; Gao, J.; Hummelen, J. C.; Wudl, F.; Heeger, A. J. *Science* **1995**, *270*, 1789−1791.

(3) Günes, S.; Neugebauer, H.; Sariciftci, N. S. *Chem. Rev.* **2007**, *107*, 1324−1338.

(4) Thompson, B. C.; Fréchet, J. M. J. *Angew. Chem., Int. Ed.* **2008**, *47*, 58−77.

(5) Cheng, Y.-J.; Yang, S.-H.; Hsu, C.-S. *Chem. Rev.* **2009**, *109*, 5868−5923.

(6) He, Y.; Li, Y. *Phys. Chem. Chem. Phys.* **2011**, *13*, 1970−1983.

(7) Li, C.-Z.; Yip, H.-L.; Jen, A. K.-Y. *J. Mater. Chem.* **2012**, *22*, 4161−4177.

(8) Green, M. A.; Emery, K.; Hishikawa, Y.; Warta, W.; Dunlop, E. D. *Prog. Photovolt.: Res. Appl.* **2013**, *21*, 827−837.

(9) Chen, H.-Y.; Hou, J.; Zhang, S.; Liang, Y.; Yang, G.; Yang, Y.; Yu, L.; Wu, Y.; Li, G. *Nat. Photonics* **2009**, *3*, 649−653.

(10) Brabec, C. J.; Cravino, A.; Meissner, D.; Sariciftci, N. S.; Fromherz, T.; Rispens, M. T.; Sanchez, L.; Hummelen, J. C. *Adv. Funct. Mater.* **2001**, *11*, 374−380.

(11) Scharber, M. C.; Mühlbacher, D.; Koppe, M.; Denk, P.; Waldauf, C.; Heeger, A. J.; Brabec, C. J. *Adv. Mater.* **2006**, *18*, 789−794.

(12) Koster, L. J. A.; Mihailetchi, V. D.; Blom, P. W. M. *Appl. Phys. Lett.* **2006**, *88*, 093511−1−093511−3.

(13) Kooistra, F. B.; Knol, J.; Kastenberg, F.; Popescu, L. M.; Verhees, W. J. H.; Kroon, J. M.; Hummelen, J. C. *Org. Lett.* **2007**, *9*, 551−554.

(14) Zhang, Y.; Yip, H.-L.; Acton, O.; Hau, S. K.; Huang, F.; Jen, A. K.-Y. *Chem. Mater.* **2009**, *21*, 2598−2600.

(15) Yang, C.; Kim, J. Y.; Cho, S.; Lee, J. K.; Heeger, A. J.; Wudl, F. *J. Am. Chem. Soc.* **2008**, *130*, 6444−6450.

(16) Backer, S. A.; Sivula, K.; Kavulak, D. F.; Fréchet, J. M. J. *Chem. Mater.* **2007**, *19*, 2927−2929.

(17) Lenes, M.; Wetzelaer, G.-J. A. H.; Kooistra, F. B.; Veenstra, S. C.; Hummelen, J. C.; Blom, P. W. M. *Adv. Mater.* **2008**, *20*, 2116−2119.

(18) He, Y.; Chen, H.-Y.; Hou, J.; Li, Y. *J. Am. Chem. Soc.* **2010**, *132*, 1377−1382.

(19) Cheng, Y.-J.; Hsieh, C.-H.; He, Y.; Hsu, C.-S.; Li, Y. *J. Am. Chem. Soc.* **2010**, *132*, 17381−17383.

(20) Zhao, G.; He, Y.; Li, Y. *Adv. Mater.* **2010**, *22*, 4355−4358.

(21) Ye, G.; Chen, S.; Xiao, Z.; Zuo, Q.; Wei, Q.; Ding, L. *J. Mater. Chem.* **2012**, *22*, 22374−22377.

(22) Han, G. D.; Collins, W. R.; Andrew, T. L.; Bulović, V.; Swager, T. M. *Adv. Funct. Mater.* **2013**, *23*, 3061−3069.

(23) Liu, C.; Xu, L.; Chi, D.; Li, Y.; Liu, H.; Wang, J. *ACS Appl. Mater. Interfaces* **2013**, *5*, 1061−1069.

(24) Kim, K.-H.; Kang, H.; Nam, O. Y.; Jung, J.; Kim, P. S.; Cho, C.-H.; Lee, C.; Yoon, S. C.; Kim, B. J. *Chem. Mater.* **2011**, *23*, 5090−5095.

(25) Li, C.-Z.; Yip, H.-L.; Jen, A. K.-Y. *J. Mater. Chem.* **2012**, *22*, 4161−4177.

(26) Ye, G.; Chen, S.; Xiao, Z.; Zuo, Q.; Wei, Q.; Ding, L. *J. Mater. Chem.* **2012**, *22*, 22374−22377.

(27) Zhang, C.; Chen, S.; Xiao, Z.; Zuo, Q.; Ding, L. *Org. Lett.* **2012**, *14*, 1508−1511.

(28) Cheng, Y.-J.; Liao, M.-H.; Chang, C.-Y.; Kao, W.-S.; Wu, C.-E.; Hsu, C.-S. *Chem. Mater.* **2011**, *23*, 4056−4062.

(29) Li, C.-Z.; Chien, S.-C.; Yip, H.-L.; Chueh, C.-C.; Chen, F.-C.; Matsuo, Y.; Nakamura, E.; Jen, A. K.-Y. *Chem. Commun.* **2011**, *47*, 10082−10084.

(30) He, Y.; Peng, B.; Zhao, G.; Zou, Y.; Li, Y. *J. Phys. Chem. C* **2011**, *115*, 4340−4344.

(31) Meng, X.; Zhang, W.; Tan, Z.; Li, Y.; Ma, Y.; Wang, T.; Jiang, L.; Shu, C.; Wang, C. *Adv. Funct. Mater.* **2012**, *22*, 2187−2193.

(32) Kim, K.-H.; Kang, H.; Kim, H. J.; Kim, P. S.; Yoon, S. C.; Kim, B. J. *Chem. Mater.* **2012**, *24*, 2373−2381.

(33) Hirsch, A.; Lamparth, I.; Karfunkel, H. R. *Angew. Chem., Int. Ed.* **1994**, *33*, 437−438.

(34) Kitaura, S.; Kurotobi, K.; Sato, M.; Takano, Y.; Umeyama, T.; Imahori, H. *Chem. Commun.* **2012**, *48*, 8550−8552.

(35) Bouwer, R. K. M.; Hummelen, J. C. *Chem.—Eur. J.* **2010**, *16*, 11250−11253.

(36) Bouwer, R. K. M.; Wetzelaer, G. -J.; Blom, P. W. M.; Hummelen, J. C. *J. Mater. Chem.* **2012**, *22*, 15412−15417.

(37) Lenes, M.; Shelton, S. W.; Sieval, A. B.; Kronholm, D. F.; Hummelen, J. C.; Blom, P. W. M. *Adv. Funct. Mater.* **2009**, *19*, 3002−3007.

(38) Frost, J. M.; Faist, M. A.; Nelson, J. *Adv. Mater.* **2010**, *22*, 4881−4884.

(39) Azimi, H.; Senes, A.; Scharber, M. C.; Hingerl, K.; Brabec, C. J. *Adv. Energy Mater.* **2011**, *1*, 1162−1168.

(40) Diederich, F.; Kessinger, R. *Acc. Chem. Res.* **1999**, *32*, 537−545.

(41) Bourgeois, J.-P.; Echegoyen, L.; Fibbioli, M.; Pretsch, E.; Diederich, F. *Angew. Chem., Int. Ed.* **1998**, *37*, 2118−2121.

(42) Taki, M.; Sugita, S.; Nakamura, Y.; Kasashima, E.; Yashima, E.; Okamoto, Y.; Nishimura, J. *J. Am. Chem. Soc.* **1997**, *119*, 926−932.

(43) Isaacs, L.; Haldimann, R. F.; Diederich, F. *Angew. Chem., Int. Ed.* **1994**, *33*, 2339−2342.

(44) Nierengarten, J.-F.; Gramlich, V.; Cardullo, F.; Diederich, F. *Angew. Chem., Int. Ed.* **1996**, *35*, 2101−2103.

(45) Ashton, P. R.; Diederich, F.; Gomez-Lopez, M.; Nierengarten, J.-F.; Preece, J. A.; Raymo, F. M.; Stoddart, J. F. *Angew. Chem., Int. Ed.* **1997**, *36*, 1448−1451.

(46) Dietel, E.; Hirsch, A.; Eichhorn, E.; Rieker, A.; Hackbarth, S.; Röder, B. *Chem. Commun.* **1998**, 1981−1982.

(47) Atkinson, G. E.; Fischer, P. M.; Chan, W. C. *J. Org. Chem.* **2000**, *65*, 5048−5056.

(48) Nakamura, Y.; Takano, N.; Nishimura, T.; Yashima, E.; Sato, M.; Kudo, T.; Nishimura, J. *Org. Lett.* **2001**, *3*, 1193−1196.